Colloidal Interactions between Particles with Tethered Nonpolar Chains Dispersed in Polar Media: Direct Correlation between Dynamic Rheology and Interaction Parameters

Srinivasa R. Raghavan,[†] Jun Hou,[‡] Gregory L. Baker,[‡] and Saad A. Khan*[,†]

Department of Chemical Engineering, North Carolina State University, Raleigh North Carolina 27695-7905, and Department of Chemistry, Michigan State University, East Lansing, Michigan 27689

Received November 13, 1998. In Final Form: September 7, 1999

Colloidal interactions between particles dispersed in a liquid can be suitably tailored by modifying the surface chemistry of the particles. In the case of fumed silica particles, the surface can be systematically altered from hydrophilic to hydrophobic by replacing a portion of the original silanol (Si−OH) groups by nonpolar alkyl chains. In this study, we probe the effect of surface modification of fumed silica on their rheology and microstructure in polar media. Variables of interest include the length of the tethered alkyl chain and the extent of surface coverage. For the continuous phase, we examine a range of polyether liquids comprising different architectures and molecular weights. We find that when the alkyl chains are C_8 or longer, and are attached at saturation levels, a dense nonpolar surface layer is formed on each silica unit. Such particles experience strong interactions in polar media, leading to the formation of a volume-filling network (gel). We show that these interactions arise as a result of the negative free energy of mixing between the tethered chains, owing to the mismatch in chemical nature between chains and solvent. In this flocculation process van der Waals interactions between the particles play a negligible role. We also find that the greater the mismatch between particle surface and liquid, the greater the "stickiness" of the surface chains and correspondingly, the higher the elastic modulus (G') of the fumed silica network. This leads to a unique correlation between G' and a term comprising the χ parameter for the chain-solvent pair. An approximate but useful form of this correlation can be written as $G' \sim (\delta_s - \delta_m)^2$ where the latter expression characterizes the mismatch in solubility parameters between the surface chains (δ_s) and the liquid medium (δ_m).

A. Introduction

Colloidal particles are utilized in a wide variety of applications ranging from the established (e.g., coatings and printing inks) to the emerging (e.g., display devices and fiber-optic cable gels). In many of these applications, the particles are dispersed in a given liquid with the aim of suitably modifying the flow properties (rheology) of the system. The desired effects may include an increase in viscosity, as well as shear-thinning and thixotropy. In certain cases, it is intended for the particles to flocculate and form a colloidal gel that can exhibit elastic (solidlike) character. Thus, gel formation is often desirable and critical to the utilization of the colloidal system, as is the case in the present investigation.

In our study we use fumed silica particles[1−3] as a gelling agent in polar organic liquids. Our interest in this class of materials stems from their potential application as *composite polymer electrolytes* in rechargeable lithium batteries.[4,5] For this purpose, the organic liquids envisioned for use mainly belong to the polyether family: for example, poly(ethylene glycol) (PEG) and poly(propylene glycol) (PPG). Solutions of polyether and lithium salt serve as polymer electrolytes owing to the unique capability of the polyether chain to solvate small cations such as lithium (Li^+).[6] On addition of an appropriately chosen fumed silica, one can transform the liquid solution into a free-standing gel,[4] thus offering a highly conductive electrolyte with solidlike characteristics.

The extent of thickening (rise in viscosity and/or gelation) on adding colloidal particles to a liquid is largely dependent on the surface chemistry of the particles. Conventional fumed silica is hydrophilic, having a surface covered with silanol (Si−OH) groups.[1] This type of silica is largely incapable of gelling polar organic liquids such as alcohols or ethers.[2] On the other hand, a fumed silica which is rendered hydrophobic by attaching nonpolar groups to the particle surface can establish a volume-filling network structure (gel) in polar liquids.[2,4,7,8] In this study we attempt to elucidate the colloidal interactions responsible for gel formation in the latter systems. We use a range of hydrophobic fumed silicas derived by

* Corresponding author. Phone: (919) 515-4519. Fax: (919) 515-3465. E-mail: khan@eos.ncsu.edu.

[†] North Carolina State University.

[‡] Michigan State University.

(1) *Basic Characteristics of Aerosil*; Degussa Technical Bulletin No. 11; Degussa Corp.: Akron, OH, 1993.

(2) *Aerosil as a Thickening Agent for Liquid Systems*; Degussa Technical Bulletin No. 23; Degussa Corp.: Akron, OH, 1993.

(3) Barthel, H.; Rosch, L.; Weis, J. Fumed Silica: Production, Properties and Applications. In *Organosilicon Chemistry II*: *From Molecules to Materials*; Auner, N., Weis, J., Eds.; VCH Publishers: Weinheim, Germany, 1996.

(4) Raghavan, S. R.; Riley, M. W.; Fedkiw, P. S.; Khan, S. A. Composite Polymer Electrolytes Based on Poly(ethylene glycol) and Hydrophobic Fumed Silica: Dynamic Rheology and Microstructure. *Chem. Mater.* **1998**, *10*(*1*), 244−251.

(5) Hou, J. Composite Polymer Electrolytes Using Functionalized Fumed Silica and Low Molecular Weight PEO: Synthesis and Characterization Ph.D. Thesis, Michigan State University, 1997.

(6) Gray, F. M. *Solid Polymer Electrolytes*: *Fundamentals and Technological Applications*; VCH Publishers: New York, 1991.

(7) *Hydrophobic AEROSIL*: *Manufacture, Properties and Applications*; Degussa Technical Bulletin No. 6; Degussa Corp.: Akron, OH, 1991.

(8) *The Use of Hydrophobic Aerosil in the Coatings Industry*; Degussa Technical Bulletin No. 18; Degussa Corp.: Akron, OH, 1993.

10.1021/la9815953 CCC: $19.00
Published on Web 11/27/1999

attaching nonpolar alkyl chains (of length C_2 to C_{18}) to the silica surface. These silicas are studied in a variety of polar organic liquids, our main interest being in liquids belonging to the glycol (polyether) family. We therefore examine a range of polyether liquids (PEGs, PPGs) of various molecular weights (well below the entanglement limit in all instances) and end functionalities. In accordance with our fundamental objectives, we restrict our study to two-component systems (silica dispersed in a given liquid). Studies on typical composite electrolytes (silica + liquid + lithium salt) are reported elsewhere.[4]

The ability of hydrophobic fumed silicas to act as thickening agents in polar media is quite well-known, and is described in technical brochures provided by the manufacturer.[2,7,8] However, the exact basis for this effect is poorly understood. As a result, no predictive capability exists at this point to estimate the extent of thickening obtained with a particular silica, or to distinguish between the thickening abilities of different grades (surface chemistries) of hydrophobic silicas. Consequently, practical tests are unavoidable for optimizing formulations.[7,8] A limited number of systematic studies have been conducted with hydrophobic fumed silicas in polar organic liquids.[9−14] Much of the information reported in these studies is rheological; typically, the steady shear viscosity of the dispersion is reported at a constant shear rate.[10,12] Note, however, that in these systems, the silica typically flocculates and/or forms a gel, and hence the viscosity will be shear thinning. Thus, the viscosity at a given shear rate is *not* a characteristic parameter, and cannot be correlated readily with either the prevailing microstructure or with the attendant colloidal interactions. Therefore, limited insight can be obtained from the earlier work regarding the fundamental behavior of these systems.

The technique of hydrophobicizing particles by grafting alkyl chains has been extensively utilized not only for fumed silicas, but also for other forms of colloidal silica, such as that obtained by the Stober method.[15−20] For instance, Stober silica particles grafted with C_{18} (octadecyl) chains have been studied in a range of nonpolar organic liquids (*n*-alkanes, cyclohexane, etc.).[17−20] These systems are interesting from a rheological point of view because they can act as true hard-sphere dispersions, thus enabling the verification of rheological theories.[20] However, to our knowledge, no studies have been performed using these silicas in *polar* liquids.

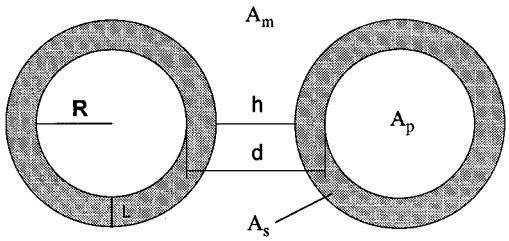

Figure 1. Schematic representation of spherical particles bearing a homogeneous surface layer of thickness *L*. Subscripts p, s, and m refer to the particle, the surface layer, and the continuous medium, respectively.

From a broader perspective, the problem we are dealing with concerns the interaction forces between colloidal particles having a surface layer of different chemical constitution. Qualitatively, it is easy to understand why particles with tethered surface layers flocculate to form gels in certain liquids. This typically occurs when there is a *mismatch between the chemical nature of the particle surface and that of the liquid*.[3,21] Thus when the particle surfaces are rendered nonpolar, and the dispersion medium is polar, there will be a tendency for the nonpolar surfaces to associate. Such interparticle associations, when extended throughout the sample volume, result in gel formation. The above qualitative reasoning, however, fails to address several fundamental questions, such as:

(1) What is the exact nature and origin of the interparticle forces?

(2) What measurable properties of the core particles, the tethered surface layer, and the liquid, can be correlated with the intensity of these interparticle forces?

The motivation behind our study is to shed some light on these issues, while at the same time obtaining practical information relevant to fumed silica systems. In the next section, we briefly review the literature dealing with colloidal interactions between particles having molecules (chains) terminally attached to their surfaces.

Colloidal Interactions between Particles with Surface Layers. *a. van der Waals Interactions.* We first consider the effect of surface layers on the van der Waals (vdW) attractive forces between particles. The problem was originally analyzed by Vold[22] and later refined by Vincent.[23,24] We present below the equations derived by Vold for the vdW interaction potential between two spherical particles of radius *R*, each having a surface layer (e.g., of terminally anchored chains). The situation is depicted schematically in Figure 1. The layer thickness is denoted by *L* and the minimum distance of separation between the outer boundaries of the layers is denoted by *h*. Subscripts p, s, and m will henceforth refer to the particle, the surface layer, and the continuous medium, respectively. The minimum separation distance between the *core* particles is given by *d* where

(9) Benitez, R.; Contreras, S.; Goldfarb, J. Dispersions of Methylated Silica in Mixed Solvents. *J. Colloid Interface Sci.* **1971**, *36*, 146−150.

(10) Lee, G.; Rupprecht, H. Rheological Properties of Nonmodified and *n*-alkyl Surface Modified Colloidal Silica Sols. *J. Colloid Interface Sci.* **1985**, *105*, 257−266.

(11) Lee, G.; Murray, S.; Rupprecht, H. The Dispersion of Hydrophilic and Hydrophobic Flame-Hydrolyzed Silicas in Short-Chained Alkanols. *Colloid Polymer Sci.* **1987**, *265*, 535−541.

(12) Jiao, W.; Vidal, A.; Papirer, E.; Donnet, J. B. Modification of Silica Surfaces by Grafting of Alkyl Chains. III. Particle/Particle Interactions: Rheology of Silica Suspensions in Low Molecular Weight Analogues of Elastomers. *Colloids Surf.* **1989**, *40*, 279−291.

(13) Sawan, S. P.; Muni, K. P.; Svelnis, S. M. Viscometric Properties of Phenoxy Solutions Containing Hydrophilic or Hydrophobic Fumed Silica. *Polymer Preprints* **1991**, *32*, 187.

(14) Barthel, H. Surface Interactions of Dimethylsiloxy Group-Modified Fumed Silica. *Colloids Surf.* **1995**, *101*, 217−226.

(15) Iler, R. K. *The Chemistry of Silica*: *Solubility, Polymerization, Colloid and Surface Properties, and Biochemistry*; John Wiley & Sons: New York, 1979.

(16) Rothon, R. Surface Modification and Surface Modifiers. In *Particulate-Filled Polymer Composites*; Rothon, R., Ed.; Longman Scientific: Harlow, England, 1995.

(17) Vincent, B. The Stability of Nonaqueous Dispersions of Weakly Interacting Particles. *Colloids Surf.* **1987**, *24*, 269−282.

(18) Chen, M.; Russel, W. B. Characteristics of Flocculated Silica Dispersions. *J. Colloid Interface Sci.* **1991**, *141*, 564−577.

(19) Rouw, P. W.; Vrij, A.; De Kruif, C. G. Adhesive Hard-Sphere Colloidal Dispersions III. Stickiness in n-Dodecane and Benzene. *Colloids Surf.* **1988**, *31*, 299−309.

(20) Woutersen, A. T. J. M.; Mellema, J.; Blom, C.; De Kruif, C. G. Linear Viscoelasticity in Dispersions of Adhesive Hard Spheres. *J. Chem. Phys.* **1994**, *101*, 542−553.

(21) Israelachvili, J. *Intermolecular and Surface Forces* 2nd ed.; Academic Press: San Diego, CA, 1991.

(22) Vold, M. J. The Effect of Adsorption on the van der Waals Interaction of Spherical Colloidal Particles. *J. Colloid Sci.* **1961**, *16*, 1−12.

(23) Osmond, D. W. J.; Vincent, B.; Waite, F. A. The van der Waals Attraction Between Colloid Particles Having Adsorbed Layers: I. A Reappraisal of the Vold Effect. *J. Colloid Interface Sci.* **1973**, *42*, 262−269.

(24) Vincent, B. The van der Waals Attraction Between Colloid Particles Having Adsorbed Layers: II. Calculation of Interaction Curves. *J. Colloid Interface Sci.* **1973**, *42*, 270−285.

$$d = h + 2L \tag{1}$$

The free energy for vdW interaction V_{vdW} as a function of the distance h between the layers is given below in the limit $h \ll R$[22,25]

$$V_{vdW} = -\frac{R}{12}\left[\frac{(\sqrt{A_m} - \sqrt{A_s})^2}{h} + \frac{(\sqrt{A_s} - \sqrt{A_p})^2}{h + 2L} + \frac{(\sqrt{A_m} - \sqrt{A_s})(\sqrt{A_s} - \sqrt{A_p})}{h + L}\right] \tag{2}$$

Here A_p, A_s, and A_m refer to the Hamaker constants of the particle, the surface layer, and the continuous medium, respectively. In the absence of the surface layer, the vdW potential between the core particles, denoted by V^0_{dw}, evaluated at the same distance of separation between the core particles, i.e., d, is given by

$$V^0_{dw} = -\frac{R}{12d}[(\sqrt{A_m} - \sqrt{A_p})^2] \tag{3}$$

From the above equations, we can see that under certain conditions (e.g., $A_m > A_p \gg A_s$), the van der Waals potential V_{vdW} will be greater than V^0_{dw}, i.e., the vdW interaction will be enhanced due to the presence of the surface layer.[22,23]

b. Steric Interactions. The effect of a layer of tethered chains on colloidal particles has been studied extensively from the viewpoint of steric stabilization, i.e., concerning the ability of the chains (usually polymeric) to provide thermodynamic stability to the particles in a dispersion.[26−31] Stability implies a net repulsive pair-potential V_{steric} between the polymer-covered particles. Our interest lies in the opposite scenario, where the potential V_{steric} is attractive, thereby causing the particles to flocculate into a colloidal gel. Compared to the vdW interaction, the steric interaction is much more short-ranged, and begins to operate only at distances corresponding to the overlap of the surface layers (i.e., $d < 2L$, same geometry as in Figure 1). Furthermore, two regimes are usually distinguished:[26]

(Zone 1)

$L < d < 2L$: chains undergo interpenetration

(Zone 2)

$d < L$: chains undergo compression + interpenetration

The main governing parameter which dictates the sign of V_{steric} is the affinity (or lack thereof) between the solvent and the tethered chains. This aspect is brought out clearly in the relatively simple theory of Napper and co-workers.[27,29] In this approach, two separate contributions to the steric interaction potential V_{steric} are distinguished: the *mixing* or osmotic contribution ΔG_{mix} arising due to the intimate mixing of chain segments from two different particles, and the *elastic* contribution ΔG_{el} which accounts for the entropy loss due to the constriction of the chains between the rigid particle surfaces. Thus,

$$V_{steric} = \Delta G_{mix} + \Delta G_{el} \tag{4}$$

In the following analysis, our emphasis will be on the interpenetration zone, because we expect the destabilization of particles to be initiated in this zone. In this zone, the elastic term ΔG_{el} is zero. (The contribution of ΔG_{el} is only to add a steep repulsive potential in the compression zone which ensures that the particles cannot approach beyond a certain point.) Thus the steric interaction potential ($V_{steric} \equiv \Delta G_{mix}$) in the interpenetration zone ($L < d < 2L$) between two identical spherical particles is as follows[29]

$$\frac{V_{steric}}{kT} = \left[\frac{4\pi R}{v_m}\phi^{av}(L - d/2)^2\right]\left(\frac{1}{2} - \chi\right) \tag{5}$$

where R is the particle radius, k is the Boltzmann constant, T is the absolute temperature, v_m is the volume of a solvent molecule, and χ is the Flory−Huggins interaction parameter. The term ϕ^{av} is the average volume fraction of segments in the grafted layer. In deriving eq 5 the segment density is assumed to obey a step profile, with a uniform segment density ($\approx\phi^{av}$) in the layer and a sharp decrease to zero outside the layer. This distribution is considered to be an adequate approximation for the case of short, terminally anchored chains of identical molecular weight.[29,32]

It is evident from eq 5 that the sign of V_{steric} depends only on the value of the χ parameter (since the expression within square brackets is always positive). The Flory−Huggins interaction parameter χ represents the solvency of the medium for the chain segments.[33] To stabilize particles (positive V_{steric}), the medium must be a good solvent for the chains, i.e., χ should be $< {}^1/_2$. Alternately, in poor solvents $\chi \gg {}^1/_2$ leading to attractive interactions (negative V_{steric}) which cause particles to flocculate. In our systems, we consider a variety of liquid media of varying solvent quality for our tethered chains. If we assume that the major effect on changing the solvent is on the value of the χ parameter, we can deduce from eq 5 the following scaling relation

$$\frac{V}{kT} \sim \left(\frac{1}{2} - \chi\right) \tag{6}$$

Note that χ is an empirical but experimentally measurable parameter. A convenient way to estimate χ for a two-component system (polymer s in a solvent medium m) is by using the solubility parameter approach.[33,34] The resulting expression is:

$$\chi = \frac{V_m}{RT}(\delta_s - \delta_m)^2 + 0.34 \tag{7}$$

(25) Vincent, B.; Kiraly, Z.; Emmett, S.; Beaver, A. The Stability of Silica Dispersions in Ethanol/Cyclohexane Mixtures. *Colloids Surf.* **1990**, *49*, 121−132.

(26) Vincent, B. The Effect of Adsorbed Polymers on Dispersion Stability. *Adv. Colloid Interface Sci.* **1974**, *4*, 193−277.

(27) Napper, D. H. Steric Stabilization. *J. Colloid Interface Sci.* **1977**, *58*, 390−407.

(28) Vincent, B.; Whittington, S. G. Polymers at Interfaces and in Disperse Systems. In *Surface and Colloid Science*; Matjevic, E., Ed.; Plenum Press: New York, 1982; Vol. 12.

(29) Buscall, R.; Ottewill, R. H. The Stability of Polymer Latices. In *Polymer Colloids*; Buscall, R., Ed.; Elsevier, Amsterdam, 1985.

(30) Russel, W. B.; Saville, D. A.; Schowalter, W. R. *Colloidal Dispersions*; Cambridge University Press: New York, 1989.

(31) Zhulina, E. B.; Borisov, O. V.; Priamitsyn, V. A. Theory of Steric Stabilization of Colloid Dispersions by Grafted Polymers. *J. Colloid Interface Sci.* **1990**, *137*, 495−511.

(32) Bagchi, P. On the Assumption of a Step Function for the Adsorption-Layer Thickness in the Nonionic Stabilization of Dispersions. *J. Colloid Interface Sci.* **1975**, *50*, 115−124.

(33) Brandrup, J.; Immergut, E. H. *Polymer Handbook* , 3rd ed.; John Wiley & Sons: New York, 1989.

(34) Du, Y.; Xue, Y.; Frisch, H. L. Solubility Parameters. In *Physical properties of Polymers Handbook*; Mark, J. E., Ed.; AIP Press: New York, 1996.

Here V_m is the molar volume of the solvent medium, and δ_s and δ_m are the solubility parameters of the polymer s and solvent medium m respectively. The solubility parameter is a measure of the cohesive energy density of the component in its condensed phase.[34] We find from eq 7 that if the solubility parameter for the grafted layer in its condensed phase (δ_s) is significantly different from that of the medium (δ_m), it then follows that the χ parameter will be significantly greater than $^1/_2$, thus leading to a negative steric potential and hence to attractive interactions between the grafted particles.

Utility of Dynamic Rheology in Probing Colloidal Interactions. To probe the microstructure and hence the colloidal interactions in our dispersions, we resort to dynamic rheology. This technique is particularly useful because we can probe the materials in their equilibrium state, without causing disruption of their underlying structures.[35] The frequency spectrum for a given system, i.e., the variation of elastic modulus (G') and viscous modulus (G'') with oscillation frequency, provides a signature of the at-rest microstructure existing in the system.[30,36] Most of our dispersions are colloidal gels and hence essentially display elastic behavior: their elastic modulus G' is independent of frequency and dominates over the viscous modulus G''. Thus the frequency-independent value of G' (which can alternately be called the gel modulus) can be used as a characteristic parameter of the gel.[36]

We now need to relate G' to the colloidal interactions responsible for gel formation. To obtain a quantitative expression for G' we also require structural (geometric) details of the individual particles and the network itself. As has been vividly demonstrated in recent years, the internal structures in colloidal gels are extremely complex and show self-similarity (fractal geometry).[37] To confound matters further, the primary units of fumed silica are not regular spherical particles, but aggregates of such particles.[1,2] Due to these complications, we restrict ourselves to simple scaling relationships for G' that incorporate only interaction parameters.[30,38−40] For this we will assume that the structural and colloidal contributions to G' can be separated out.[30] In our analysis, the network is considered to be a collection of linked units, with each link being the result of a colloidal pair potential $V(h)$.[36] The number of links in the network per unit volume is denoted by N, and pairwise additivity of the links is assumed. One can then relate G' to $V(h)$ by the following expression[30,39]

$$G' \sim N \cdot \frac{d^2V}{dh^2}(h_{min})$$

$$\text{i.e., } G' \sim N \cdot V''_{min} \qquad (8)$$

The above equation states that the gel modulus G' is related to the second derivative of the pair potential $V(h)$. This derivative is evaluated at $h = h_{min}$ which corresponds to the equilibrium distance between any two particles—hence the notation V''_{min}. We can then use eq 8 in conjunction with an appropriate equation for the interaction potential (such as eq 2 or eq 5), and thus relate the gel modulus to interaction parameters.

In the above equation, the parameter N, which represents the number of (identical) links in the network, will be a function of the particle volume fraction ϕ_p. Since the geometric details of our system are complicated, the dependence of N (and hence G') on the volume fraction ϕ_p cannot be elucidated easily, and this aspect is therefore ignored in our analysis. Thus the above scaling relationship for G' is only valid at a constant particle volume fraction. In addition, it has been postulated that N may also depend on the pair potential itself (i.e., the stronger the attraction, the greater the number of network links per unit volume).[30] However, for this assumption to be valid, some local equilibration of the structure must take place to allow the nearest neighbors to respond to the strength of the attraction. Since gels are metastable structures, such equilibration is unlikely, and therefore, it is more likely that N is determined solely by geometric or kinetic considerations, especially for high particle concentrations.

The use of dynamic rheology in our study is a considerable improvement over previous studies on fumed silica systems, which employed only steady shear rheology.[10−14] These previous studies could often be misleading and do not offer a suitable basis for comparing different systems. Note also that the application of steady shear involves the disruption of structures present at rest. For colloidal gels, the gel modulus (G') is the most meaningful rheological parameter to use in characterizing a system.[39] This is because G' is a static parameter so that its correlation with the interaction potential is more direct, unlike parameters such as the viscosity which require the solution of hydrodynamic equations. Therefore, we use dynamic rheology to obtain insight into the mechanisms responsible for gel formation in fumed silica systems. Preliminary studies conducted in our laboratories provide a starting point for this investigation.[41−43] Our goal is to understand colloidal factors sufficiently well so as to enable rational choice of fumed silicas for any given application.

B. Experimental Section

The colloidal particulate matter used in this study is fumed silica, which is an amorphous, nonporous form of silicon dioxide (SiO_2) prepared by a flame hydrolysis process.[1,2] Its primary structure consists of branched aggregates (ca. 0.1 μm long) formed by the fusion of spherical particles (ca. 10 nm diameter). This aggregated structure is responsible for the unique properties of fumed silica. Note that the aggregates cannot be disrupted further by shear.

A total of nine different fumed silicas are used in this study, and details of their surface chemistries are provided in Table 1. The first three silicas are commercially available varieties obtained from Degussa Corp., Akron, OH. The unmodified fumed silica (A200) has a surface covered with silanols (Si−OH) to the extent of about 2.5 [SiOH] groups/nm^2, or equivalently about 0.84 mmol/g.[1,5] These silanols render the native fumed silica surface hydrophilic. The silanols can be replaced by reaction with various chlorosilanes, alkoxysilanes, or silazanes.[7,15] Each

(35) Ferry, J. D. *Viscoelastic Properties of Polymers*, 3rd ed.; John Wiley & Sons: New York, 1980.
(36) Russel, W. B. "Theoretical approaches to the Rheology of Concentrated Dispersions. *Powder Technol.* **1987**, *51*, 15−25.
(37) Harrison, A. P. *Fractals in Chemistry*; Oxford University Press: London 1995.
(38) Tadros, T. F. Correlation of Viscoelastic Properties of Stable and Flocculated Suspensions with their Interparticle Interactions", *Adv. Colloid Interface Sci.* **1996**, *68*, 97−200.
(39) Goodwin, J. W.; Hughes, R. W.; Partridge, S. J. The Elasticity of Weakly Flocculated Suspensions. *J. Chem. Phys.* **1986**, *85*, 559.
(40) Raynaud, L.; Ernst, B.; Verge, C.; Mewis, J. Rheology of Aqueous Lattices with Adsorbed Stabilizer Layers. *J. Colloid Interface Sci.* **1996**, *181*, 11−19.
(41) Khan, S. A.; Zoeller, N. J. Dynamic Rheological Behavior of Flocculated Fumed Silica Suspensions. *J. Rheol.* **1993**, *37*, 1225−1235.
(42) Raghavan, S. R.; Khan, S. A. Shear-Induced Microstructural Changes in Flocculated Suspensions of Fumed Silica. *J. Rheol.* **1995**, *39*, 1311−1325.
(43) Raghavan, S. R.; Khan, S. A. Shear-Thickening Response of Fumed Silica Suspensions under Steady and Oscillatory Shear. *J. Colloid Interface Sci.* **1997**, *185*, 57−67.

Table 1. Characteristics of Fumed Silicas Used in This Study

fumed silica	dominant surface group(s)	fraction of surface substituted[a] (%)	fraction of unreacted Si−OH (%)
1. A200	Si−OH [silanol]	0	100
2. R974	Si−$(CH_3)_2$ [di-methyl]	50	50
3. R805	Si−C_8H_{17} [octyl]	48	52
4. ODM-42	Si−C_8H_{17} [octyl]	42	58
5. ODM-31	Si−C_8H_{17} [octyl]	31	69
6. R805-TMS	Si−C_8H_{17} [octyl]	48	15
	Si−$(CH_3)_3$ [tri-methyl]	37	
7. ETCS	Si−C_2H_5 [ethyl]	max[b]	min[b]
8. OTCS	Si−C_8H_{17} [octyl]	max[b]	min[b]
9. ODTCS	Si−$C_{18}H_{37}$ [octadecyl]	max[b]	min[b]

[a] Determined by titration using $LiAlH_4$.[5] [b] Titration by $LiAlH_4$ not possible for these silicas. Excess reactant used during synthesis to obtain maximum possible surface coverage.[5]

of the remaining fumed silicas was synthesized using A200 as the starting material (the R805-TMS silica is derived from R805 which itself is derived from A200). The primary particles of each silica are 12 nm in diameter, and the surface area of each silica is approximately 200 m^2/g. Silanol density values shown in Table 1 were determined by titration with lithium aluminum hydride ($LiAlH_4$) and are reported in detail by Hou.[5]

Synthetic procedures for silicas 4−9 in Table 3 are given in the thesis of Hou.[5] Silicas 4, 5, and 6 were specifically prepared in an attempt to vary the surface coverage of alkyl chains. The ODM-31 and ODM-42 silicas were prepared by reacting A200 with octyl dimethyl chlorosilane (ODMCS). ODM-31 showed a residual silanol density of 0.58 mmol/g, indicating that 31% of the silanols had been replaced by octyl groups and leaving 69% of the silanols unreacted. In the case of ODM-42, reaction conditions were varied so that the fraction of octyl groups was increased to 42%. This is to be compared with a figure of 48% octyl substitution in the commercially available R805 silica from Degussa. (The 48% figure represents the upper limit for octyl coverage, as the commercial product is reacted to saturation; further increases in coverage are not possible due to steric effects.[15,16]) Thus, the octyl coverage progressively increases from ODM-31 to ODM-42 to R805, thereby enabling us to study the effect of surface coverage. In an effort to further reduce the residual silanol density, the R805 silica was reacted with a small silane molecule viz. trimethylsilyl chloride (TMSCl). Thus, a portion of the unreacted silanols on the silica surface could be accessed and replaced by trimethylsilyl groups. The resulting R805-TMS silica exhibited a significantly lower residual [SiOH] density (ca. 15%) compared to the original R805 silica.

Silicas 7−9 were synthesized to systematically explore the effect of tethered chain length. The synthesis was done using three different trichlorosilanes, the abbreviations of which have been assigned to the silicas as well (ETCS, OTCS, and ODTCS are ethyl, *n*-octyl, and *n*-octadecyl trichlorosilane respectively). The *n*-alkyl moiety on the silicas thus varies from C_2 to C_8 to C_{18}. Unfortunately, the use of trichlorosilanes precludes the measurement of residual silanol density through titration methods.[15] In each case an excess of the silane was used to achieve the maximum degree of substitution by alkyl groups.[5] The success of the synthesis scheme is also qualitatively indicated as higher weight losses in TGA and as a steady increase in the intensity of C−H absorption in FTIR spectra in progressing from short (C_2) to long (C_{18}) chains.[5]

Seven different liquids were examined as part of this study (Table 2). The liquids were all low viscosity, Newtonian media. Dispersions of silica in liquid were prepared by mixing the components intensely in a Silverson SL2 mixer (Silverson Machines, Chesham, U.K.) till homogeneity was reached. Extreme care was taken to ensure good mixing quality in all our samples, since this aspect is critical to the network-forming capabilities of fumed silica.[2] The resulting dispersion was exposed to vacuum (ca. 1 kPa) at room temperature for several hours to remove entrained air bubbles. All silica concentrations are reported on a w/w (silica/liquid) basis.

Rheological experiments were conducted using a Rheometrics Dynamic Stress Rheometer (DSR-II). All experiments were run at ambient temperature (25 °C). Experiments were done using three different geometries: cone-and-plate, parallel plate, and couette (concentric cylinder), with the cone-and-plate geometry being preferred in most cases. Two different cone-and-plate fixtures were used: the larger fixture having a diameter of 40 mm and a cone angle of 0.04 rad, and the smaller fixture having a diameter of 25 mm and a cone angle of 0.1 rad. Before each dynamic experiment, a steady preshear was applied at a shear rate of 1 s^{-1} for 60 s, followed by a 120 s rest period. This procedure was necessary to erase any previous shear histories on the sample and to ensure that the sample establishes its equilibrium structure.[42]

C. Results and Discussion

Silica Surface Chemistry. We begin by contrasting the microstructure formed by hydrophilic fumed silica with that formed by typical hydrophobic fumed silicas. For this we chose a liquid that typifies the polar organic media considered here, viz. a poly(ethylene glycol) (PEG) of molecular weight 300. The behavior of three different silicas in this PEG are considered: (a) A200, which is the native, hydrophilic silica with silanol (Si−OH) groups on its surface; (b) R974, which has a di-methyl functionality on its surface; and (c) R805, which has *n*-octyl groups on its surface. The dynamic rheological response of 10% (w/w) dispersions of each silica in PEG (300) are presented in Figure 2. Each of these experiments was performed at a strain amplitude within the linear viscoelastic regime of the corresponding sample, as ascertained beforehand by strain sweep experiments.

We find that the A200 dispersion shows a primarily viscous response, with the viscous component (G'') being dominant over the entire frequency range. Moreover, both the elastic (G') and viscous (G'') moduli show a marked frequency dependence for this sample. This type of dynamic response is characteristic of a nonflocculated dispersion in which the particulate units are distinct and separated from one another. Steady shear experiments on this sample revealed a low value of the zero shear viscosity (ca. 1 Pa s) at low shear rates and a shear thickening response at higher shear rates. The rheology of hydrophilic silica dispersions is discussed in further detail elsewhere.[43,44]

In contrast, the dispersions of R974 (methyl) and R805 (octyl) silicas show a predominantly elastic response under dynamic shear (Figure 2). In each case, the moduli are frequency independent, with the elastic modulus G' exceeding the viscous modulus G'' over the frequency range. The presence of an elastic response under dynamic shear indicates that the samples are colloidal gels in which the silica units are connected together into a volume-filling network structure.[36] Thus, we find that silica particles having a polar (hydrophilic) surface are unable to flocculate in PEG, but if the silica surface is rendered nonpolar by tethering alkyl groups, the particles readily flocculate to form stable colloidal gels. Figure 2 also indicates that the elastic modulus G' for the R805 gel is more than 2 orders of magnitude higher than the G' of the R974 gel. The elastic modulus (G') of a particulate gel correlates with the rigidity (stiffness) of the network. Thus, our data implies that a much more rigid network is formed by the R805 silica which has comparatively longer chains on its surface than the R974 silica.

We now examine the effect of varying the chain length of the *n*-alkyl groups present on the fumed silica. For this

(44) Raghavan, S. R.; Khan, S. A. Rheology of Silica Dispersions in Organic Liquids: New Evidence for Solvation Forces Dictated by Hydrogen Bonding. Submitted to *Langmuir*, 1999.

Table 2. Characteristics of Liquids used in This Study

	liquid (and MW if polymeric)	molecular structure	viscosity (mPa s)
1.	triethylene glycol (EG3)	$HO-(CH_2-CH_2-O)_3-H$	37
2.	poly(ethylene glycol) (PEG) (300 g/mol)	$HO-(CH_2-CH_2-O)_n-H$ ($n \approx 6$)	69
3.	PEG methyl ether (PEG-m) (350 g/mol)	$HO-(CH_2-CH_2-O)_n-CH_3$ ($n \approx 7$)	27
4.	PEG dimethyl ether (PEG-dm) (250 g/mol)	$CH_3-O-(CH_2-CH_2-O)_n-CH_3$ ($n \approx 5$)	7
5.	poly(propylene glycol) (PPG)	$HO-[CH_2-CH(CH_3)-O]_n-H$	
	a. (425 g/mol)	($n \approx 7$)	67
	b. (1000 g/mol)	($n \approx 17$)	140
	c. (3000 g/mol)	($n \approx 51$)	580

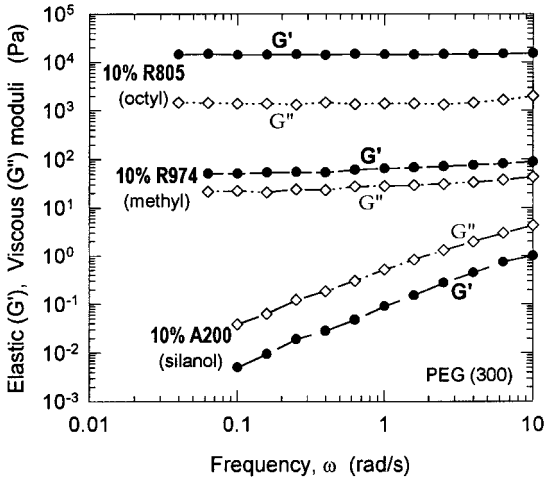

Figure 2. Dynamic rheological behavior of fumed silica dispersions in PEG (300). Data are shown for three different silicas, each bearing a different surface chemistry. The silica concentration in each case is 10% (w/w).

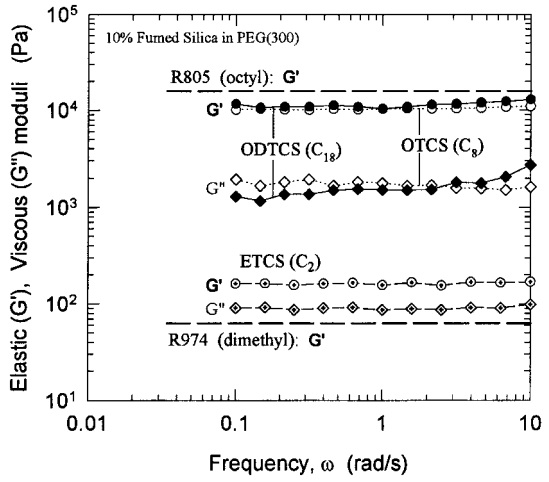

Figure 3. Effect of varying the chain length of *n*-alkyl moieties attached to the fumed silica surface. The rheology of 10% dispersions of each fumed silica in PEG (300) is shown. (See text for details.)

purpose, we used the ETCS, OTCS and ODTCS fumed silicas, in which the surface alkyl moieties varied from ethyl (C_2) to *n*-octyl (C_8) to *n*-octadecyl (C_{18}), respectively. In Figure 3, we show results for 10% dispersions of these silicas in PEG (300). We find that ETCS gives a weak gel ($G' \sim 200$ Pa), while both OTCS and ODTCS form much more rigid gels, each having a G' of about 10^4 Pa. We have also indicated the level of modulus G' obtained with gels of 10% R805 and 10% R974 (commercial fumed silicas) in the same PEG. We note that the dimethyl-functionalized R974 falls below the ETCS while the *n*-octyl-based R805 gives a value similar to the OTCS. This shows that the commercial and in-house synthesized silicas are quite comparable.

We can therefore conclude from Figure 3 that the degree of gel formation by hydrophobic fumed silicas increases with alkyl chain length, at least for short chain lengths (compare ETCS and OTCS). However, this increase only occurs up to a point which presumably corresponds to the silica surface being covered by a *dense layer* of nonpolar moieties. From the rheological data, it appears that linear chains of eight carbon atoms (*n*-octyl) are sufficient to form such a layer. Increasing the length of tethered chain beyond C_8 appears to have a negligible effect on the rheology, as evidenced by the similar moduli for the *n*-octyl (OTCS, R805) as well as *n*-octadecyl (ODTCS) silica gels. This is probably due to steric effects arising during synthesis, as a result of which the coverage obtained with C_{18} groups is expected to be lower than with C_8 groups. (In other words, the density of alkyl segments in the layer adjoining the silica surface is expected to be relatively constant at high chain lengths.) Similar results with regard to tethered chain length were found by Fox et al.[45] in their study on Stober silica dispersions.

An analogous issue is the degree of surface coverage by alkyl chains on the fumed silica. We addressed this question by comparing three different octyl-modified silicas, each having a different coverage of octyl groups. Results for R805 (48% of silanols replaced by octyl), ODM-42 (42% octyl) and ODM-31 (31% octyl), each at 10% concentration in PEG (300), are shown in Figure 4. The ODM-31 sample shows similar values for the elastic G' and viscous G'' moduli, and moreover, the moduli are both frequency-dependent. This response indicates that the ODM-31 sample is a weakly flocculated dispersion. Clearly, the octyl groups are not present in sufficient amount to shield the residual silanols which are then able to directly interact with PEG molecules (such interactions would tend to inhibit gel formation). In contrast, the ODM-42 silica with 42% octyls forms a gel having an elastic modulus G' of ~5000 Pa. This value is approximately half the modulus of the R805 gel, which has a higher coverage (48%) of octyl surface chains. From Figure 4 we can conclude that in ODM-42 the octyl layer is not dense enough to completely negate the influence of residual silanols. However, in the case of R805, the octyl layer appears to be sufficiently dense to completely screen the effects of silanol groups. Note that the degree of octyl substitution on fumed silica cannot be increased beyond the 48% figure in R805 because of steric hindrance effects from bulky octyl groups already present on the surface.[15,16]

To confirm the negligible influence of residual silanols present in R805 we examined the R805-TMS silica. This

(45) Fox, J. R.; Kokoropoulos, P. C.; Wiseman, G. H.; Bowen, H. K. Steric Stabilization of Stober Silica Dispersions Using Organosilanes. *J. Mater. Sci.* **1987**, *22*, 4528−4531.

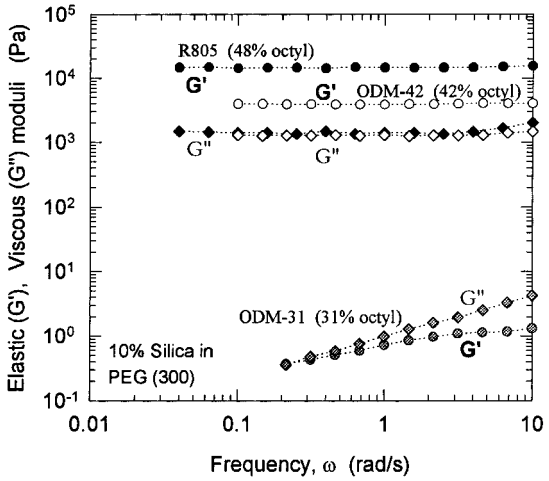

Figure 4. Effect of varying the degree of surface coverage by *n*-octyl chains on the silica. Data are shown for three silicas with different coverages dispersed in PEG (300).

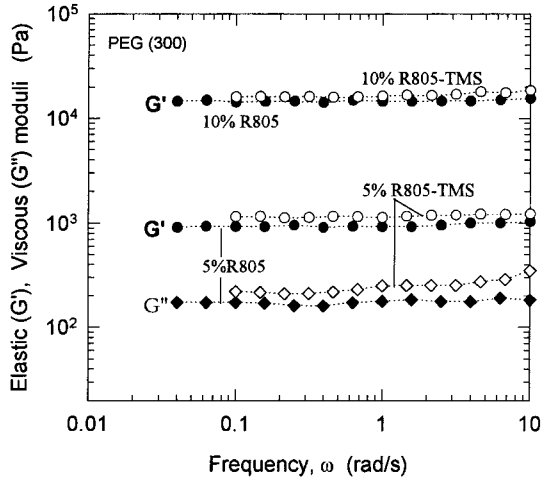

Figure 5. Effect of residual silanols present on octyl-modified fumed silica. The behavior of R805 and R805-TMS fumed silicas (with the latter having a low fraction of residual silanols) in PEG (300) are compared. For clarity, the viscous modulus (G'') is omitted in the case of the 10% silica dispersions.

silica is an analogue of R805 having a significantly lower density of residual silanols (ca. 15%), owing to reaction with trimethylsilyl chloride. (In comparison there are ca. 52% residual silanols on R805). Dynamic rheological data for dispersions of R805 and R805-TMS in PEG (300) at 5% and 10% concentrations are shown in Figure 5. We find that the gel moduli due to both silicas are virtually identical. Therefore, capping the residual silanols on R805 produces no essential difference in microstructure or aggregation patterns. Figure 5 thus confirms that the octyl chains on R805 completely swamp the surface and sterically shield the residual silanols.

Based on our rheological data, we can thus arrive at a consolidated picture of silica surface chemistry. In Figure 6a, we schematically represent the surface existing in silicas such as R805, OTCS, and ODTCS. In these silicas, the alkyl chains are assumed to adopt a relatively flat conformation and form a dense surface layer. In general, the conformation adopted by the tethered chains will depend on the solvency of the medium for the chains.[31,46] It has been shown both experimentally and theoretically

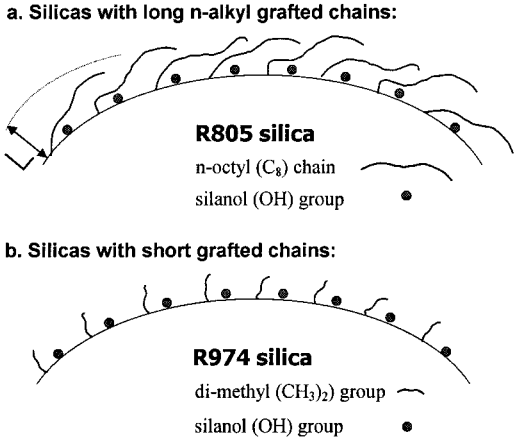

Figure 6. Schematic representation of the fumed silica surface in the case of (a) long *n*-alkyl tethered chains, as typified by the R805 silica; and (b) short tethered chains, as typified by the R974 silica.

that if the medium is a poor solvent for the surface moieties, the chain segments will tend to stay relatively close to the interface to minimize unfavorable interactions with solvent molecules.[31,46–48] This is what we expect to happen in the case of *n*-alkyl surface chains in the presence of polar liquids.[48] These *n*-alkyl chains will thereby present a steric barrier that prevents the liquid molecules from accessing the residual silanols on the underlying silica surface.

We have also schematically depicted the surface of silicas such as R974 which contain shorter alkyl chains (Figure 6b). In this case the surface exhibits a combination of polar (hydrophilic) and nonpolar (hydrophobic) character, since the smaller nonpolar groups are unable to sterically shield the silanols. A similar situation is expected in the case of long alkyl chains at low coverage (e.g., ODM-31). As we shall see, it is much more difficult to predict the rheological behavior of such silicas. In the following section, we will consider the rheology of the R805 silica (totally nonpolar surface) and the R974 silica (partially nonpolar surface) in a range of polar liquids.

Nature of Continuous Phase. We begin by examining the behavior of R805 fumed silica in the following organic ethers: triethylene glycol (EG3), poly(ethylene glycol) of molecular weight 300 (PEG (300)), and polypropylene glycol of molecular weight 425 (PPG (425)). Note that the PEG (300) and PPG (425) chains have almost an identical number of repeat units (Table 2), the only difference being the structure of the repeat unit. The dynamic rheological response of 10% R805 silica dispersions in these liquids is shown in Figure 7. All the resulting dispersions were colloidal gels ($G' > G''$, independent of frequency), and so, for clarity, we have only indicated the G'' for the PPG (425) gel. The emphasis in these studies will be on the level of the elastic modulus G', which is a measure of gel rigidity. We find that G' decreases in the order EG3 > PEG (300) > PPG (425).

The effect of PEG end-group on R805 silica dispersions is shown in Figure 8. The data are presented for 10% R805 in PEG (two −OH end-groups), PEG-m (one −OH, one $-CH_3$ end-group), and PEG-dm (two $-CH_3$ end-groups). Again, all these systems were gels and we have

(46) Cosgrove, T.; Crowley, T. L.; Ryan, K.; Webster, J. R. P. The Effects of Solvency on the Structure of an Adsorbed Polymer Layer and Dispersion Stability. *Colloids Surf.* **1990**, *51*, 255−269.

(47) Ingersent, K.; Klein, J.; Pincus, P. Interactions between Surfaces with Adsorbed Polymers: Poor Solvent. 2. Calculations and comparison with Experiment. *Macromolecules* **1986**, *19*, 1374−1381.

(48) Zeigler, R. C.; Maciel, G. E. A Study of the Structure and Dynamics of Dimethyloctadecylsilyl-Modified Silica using Wide-Line 2H NMR Techniques. *J. Am. Chem. Soc.* **1991**, *113*, 6349−6358.

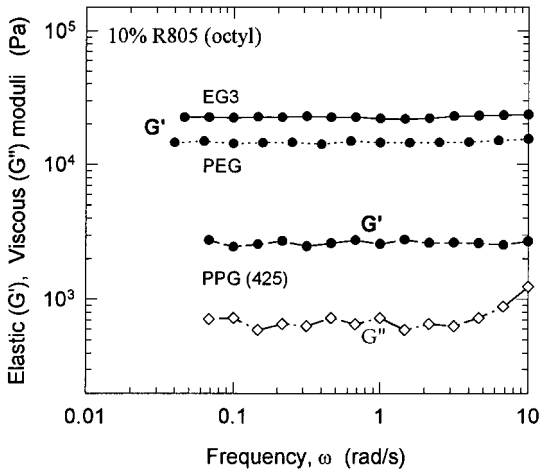

Figure 7. Rheology of R805 (*n*-octyl modified silica) in three oligoether liquids: triethylene glycol, EG3; poly(ethylene glycol), PEG (300); and polypropylene glycol, PPG (425). For clarity, the viscous modulus (G'') is shown only for the PPG system.

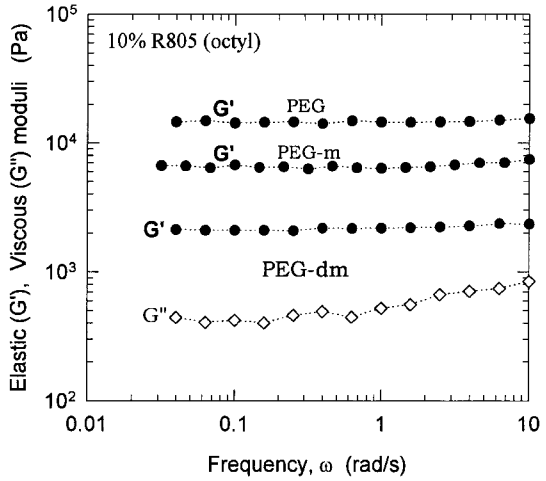

Figure 8. Effect of PEG end-group on the rheology of R805 silica dispersions. Data are shown for PEG (two −OH end-groups), PEG-m (one −OH and one $-CH_3$ end-group), and PEG-dm (two $-CH_3$ end-groups). For the sake of clarity, the viscous modulus (G'') is shown only for the dispersion in PEG-dm.

only indicated G'' for PEG-dm for the sake of clarity. We find that the elastic modulus G' of R805 gels depends quite strongly on PEG end-group, with G' decreasing in the order PEG > PEG-m > PEG-dm. Note that there is an order of magnitude difference between the moduli in PEG and PEG-dm. Thus we note that end-capping the glycol with nonpolar groups significantly reduces the gel modulus.

Next we consider the effect of polyether (PPG) molecular weight. This study was performed in PPG because it remains a liquid at ambient temperatures over a broader range of molecular weights (to ca. 5000), compared with PEG which becomes a semisolid at about 600. Results for 10% R805 dispersions in PPGs of molecular weights 425, 1000, and 3000 are presented in Figure 9. The dispersions in PPG (425) and PPG (1000) are clearly observed to be gels. However, the response of the PPG (3000) dispersion is more complicated. In the latter case G' and G'' exhibit a crossover, with G' lagging G'' at high frequencies. Toward the low end of the frequency spectrum, G' and G'' are relatively independent of frequency, and the G' curve tapers into a plateau. We can conclude that the PPG (3000) system is a flocculated dispersion that shows a semblance of gellike behavior. Figure 9 reveals that the microstructure depends strongly on polymer molecular weight. The system is transformed from a relatively strong gel in PPG (425) ($G' \approx 2500$ Pa) to a weaker gel in PPG (1000) ($G' \approx 900$ Pa) to an extremely weak or borderline gel in PPG (3000) ($G' \approx 20$ Pa).

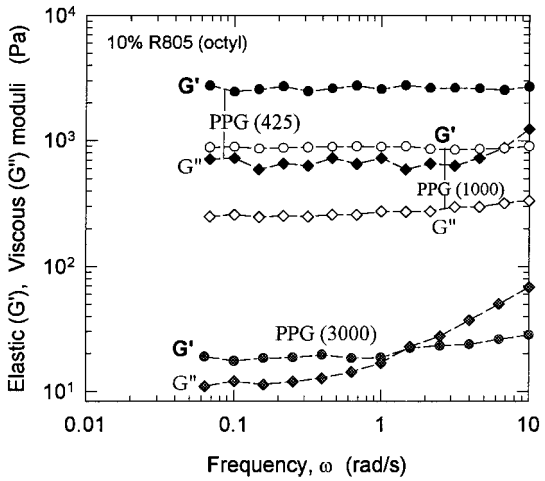

Figure 9. Effect of polyether molecular weight on the rheology of R805 silica dispersions. Data are shown for three different molecular weights of polypropylene glycol (PPG).

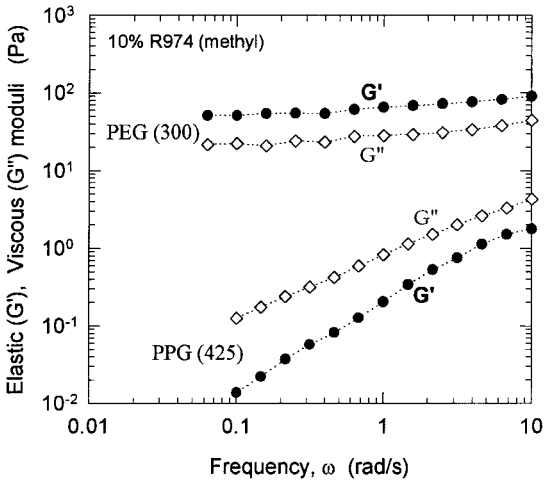

Figure 10. Rheology of R974 (methyl-terminated) fumed silica in PEG (300) and PPG (425).

We now present data for the R974 silica which, as we have indicated, is expected to show a combination of polar and nonpolar character. Data for 10% R974 dispersions in PEG (300) and PPG (425) are presented in Figure 10. We observe that the R974 silica forms a weak gel in PEG with an elastic modulus G' less than 100 Pa. In PPG on the other hand, we get a nonflocculated suspension, as evidenced by its purely viscous response. In higher molecular weight PPGs (data not shown), the R974 silica continues to form nonflocculated suspensions. On the other hand in short-chain oligomers of ethylene glycol, such as EG3, the R974 silica forms stronger gels than in PEG (300).

End-group effects with the R974 silica are indicated in Figure 11, in which dynamic data is shown for 15% R974 silica in PEG, PEG-m, and PEG-dm. We find a elastic, gellike response in PEG, a viscoelastic response in PEG-dm (indicating flocculation, but no network), and a purely viscous response in PEG-m (indicating a nonflocculated system). Note that even at 15% R974, the gel modulus G' in PEG is rather low at about 300 Pa (compared to a G' exceeding 10^4 Pa due to 10% R805 silica). In PEG-dm, a

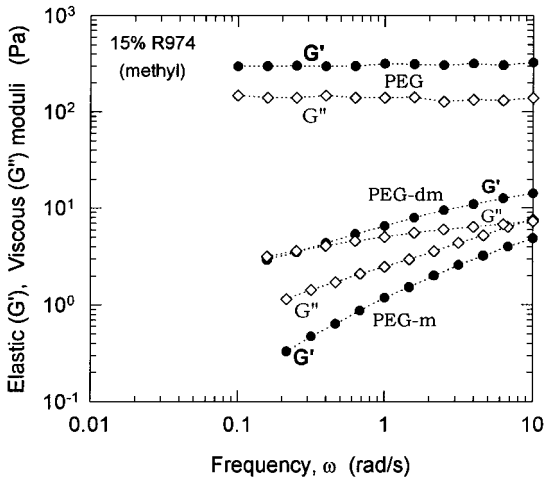

Figure 11. Effect of PEG end-group on the rheology of R974 silica dispersions. Data are shown for PEG (two −OH end-groups), PEG-m (one −OH and one $-CH_3$ end-group), and PEG-dm (two $-CH_3$ end-groups).

predominantly viscous response was obtained at lower R974 concentrations, but at 15% concentration we observe weak flocculation. We thus also find striking end-group effects in the case of R974 fumed silica.

Correlating Rheology with Colloidal Interactions. We now attempt to interpret our data through *scaling relationships* developed in terms of the colloidal interactions prevailing in our systems. In particular, the R805 silica is amenable to theoretical analysis because, as we have shown earlier, this silica may be considered to exhibit a *uniform nonpolar surface*. We first consider the van der Waals potential V_{vdW} (a logical first step in interpreting flocculation) between R805 silica units in terms of the Vold model as delineated earlier (Figure 1 and eq 2). To use this model, we will assume that the tethered *n*-octyl chains form a surface layer of pure *n*-octane on each particle. We then need estimates for the Hamaker constants (in vacuum) of the core silica particle (A_p), the surface layer of *n*-octane (A_s), and the various continuous phases (A_m). Values for these are available in the literature, or can be calculated from a knowledge of the dielectric constant (ϵ) and refractive index (n) of the material using the following equation[21]

$$A = \frac{3}{4}kT\frac{(\epsilon-1)^2}{(\epsilon+1)^2} + \frac{3h\nu_e}{16\sqrt{2}}\frac{(n^2-1)^2}{(n^2+1)^{3/2}} \qquad (9)$$

Here k is the Boltzmann constant, T is the absolute temperature, h is Planck's constant, and ν_e is the main electronic absorption frequency for the dielectric permittivity which can be taken to be 3×10^{15} s^{-1} for our media.[21] The above equation, derived using the Lifshitz theory, corresponds to the nonretarded Hamaker constant of the media in vacuum. Retardation effects are not considered because it is the potential close to the surface that is of interest. Values for the Hamaker constants of the various media determined using eq 9 are tabulated in Table 3. For the silica alone we use a different equation, obtained from ref 25. For some of the oligomeric liquid media we have used estimates for the dielectric constants, based on literature values reported for similar liquids (e.g., at other molecular weights).[4,33,49] This did not introduce significant errors into our calculations because the static contribution (first term in eq 9, due to the dielectric constants) was generally found to be negligible compared to the dispersive contribution (second term in eq 9, due to the refractive indices).

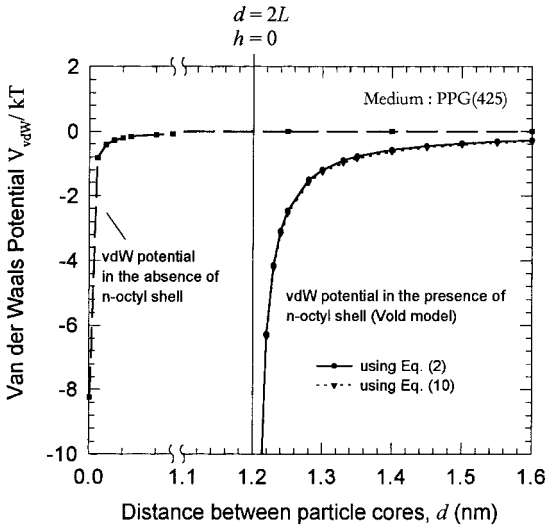

Figure 12. van der Waals potentials in PPG (425) between silica particles bearing *n*-octyl shells. Results from two different equations are plotted. The vdW potential between the bare silica particles (no shells) is also plotted.

Table 3. Bulk Parameters for Various Media

component	dielectric constant[a] ϵ	refractive index[b] n	Hamaker constant[c] at 298 K A (10^{-20} J)	solubility parameter[d] δ (MPa)$^{1/2}$
silica	3.8	1.460	6.42[e] (A_p)	—
n-octane	1.9	1.387	4.53 (A_s)	15.54
EG3	23.7	1.455	6.24	27.77
PEG (300)	15.6	1.463	6.40	24.54
PEG-m (350)	10.9	1.455	6.19	22.16
PEG-dm (250)	7.9	1.441	5.85	20.04
PPG (425)	10.1	1.447	6.01	21.21
PPG (1000)	8.1	1.449	6.03	19.88
PPG (3000)	5.7	1.451	6.04	19.27

[a] Estimated using eq 9 and using ϵ, n values from the table, except for A_p. [b] Obtained from, or estimated based on, values reported in refs 4, 33, 49. [c] As reported by the respective manufacturers. [d] Calculated using the group contribution method as detailed in refs 33, 34. [e] Calculated using equation $A_p = 15.6\ kT$ (reported in ref 25).

To calculate the van der Waals potential V_{vdW}, we need one further piece of information viz. the thickness of the *n*-octyl layer surrounding each particle. We will assume a value of $L \approx 0.6$ nm for the layer thickness, corresponding to the mean-square end-to-end distance of an *n*-octyl chain. The particle radius is taken to be the radius of a primary fumed silica particle, i.e., 6 nm. We can now estimate V_{vdW} between silica particles having an *n*-octyl layer using eq 2. Typical curves are plotted in Figure 12 for the case of PPG (425). We have also plotted the vdW interaction between the core particles V^0_{dw} in the absence of the *n*-octyl shell, and we observe that V^0_{dw} is negligibly small until the particle cores are very close to making contact ($d \approx 0$). The low value of V^0_{dw} reflects the fact that the Hamaker constants of the core silica particle (A_p) and the polyether liquids (A_m) are nearly identical. This in turn is evidently due to the close match between the refractive indices of fumed silica and the polyethers, as can be verified from Table 3. In the presence of the *n*-octyl surface layer, the vdW interaction is observed to diverge at $d = 2L$, where L is the layer thickness. The magnitude of the interaction is also considerably enhanced relative to V^0_{dw}.

(49) Van der Hoeven, P. H. C.; Lyklema, J. Electrostatic Stabilization in Nonaqueous Media. *Adv. Colloid Interface Sci.* **1992**, *42*, 205−277.

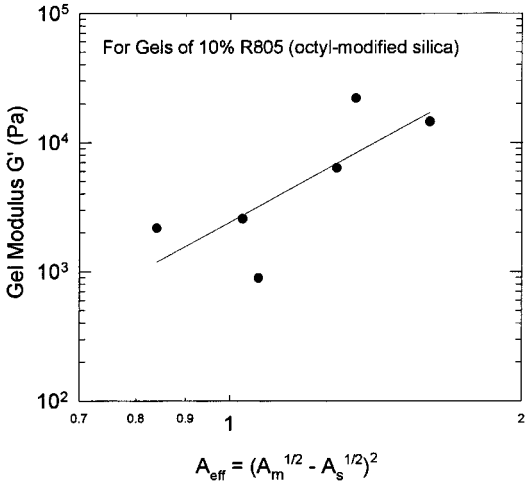

Figure 13. Test of the predicted scaling relationship between gel modulus (G') and the effective Hamaker constant A_{eff}. The data corresponds to the elastic modulus at 1 rad/s for gels of 10% R805 fumed silica in various liquids, extracted from Figures 7−9.

A closer examination of our calculations using eq 2 reveals that the last two terms are small compared to the leading term. In other words, we can approximate the vdW interaction in the presence of the *n*-octyl shell as

$$V_{vdW} = -\frac{R}{12h}[(\sqrt{A_m} - \sqrt{A_s})^2] \qquad (10)$$

To illustrate this point further, we plot V_{vdW} as given by eq 10 for the PPG(425) system in Figure 12. We find that the plot is indistinguishable from that due to eq 2, thus indicating the validity of our approximation. The foregoing analysis further confirms that it is the disparity between the surface layer (A_s) and the liquid medium (A_m) which drives the attractive vdW interaction between the particles. The term in square brackets can be considered an effective Hamaker constant A_{eff} which dictates the net vdW interaction.

We now attempt to relate the vdW potential to elastic moduli. The above expression for the vdW potential is readily differentiated and inserted into eq 8. Assuming that the equilibrium distance between particles (h_{min}) is identical in all liquids, we deduce the following scaling relationship for the gel modulus G'

$$G' \sim (\sqrt{A_m} - \sqrt{A_s})^2 = A_{eff} \qquad (11)$$

This equation indicates that the gel modulus should scale with the effective Hamaker constant A_{eff} for silica interaction in various media. We test this correlation by plotting G' for R805 gels in various liquids against A_{eff} in Figure 13. In this plot we have used experimental values for G' corresponding to gels of 10% R805 silica as shown earlier in Figures 7−9. These values are presented in decreasing order in Table 4 along with values of the corresponding A_{eff} for each silica−liquid pair. Figure 13, however, indicates only a weak correlation, if any, between G' and A_{eff}. More importantly, the data fails to predict many of the observed trends, as can be verified from Table 4; for example, A_{eff} *increases* slightly with PPG molecular weight although G' dramatically *decreases*, and likewise, A_{eff} is lower in EG3 than in PEG (300) although the reverse is true in the case of G'.

The lack of a definite correlation between G' and vdW interaction parameters suggests that the contact dissimilarity which leads to particle flocculation cannot be captured based on vdW forces alone. We now examine whether the steric mode of interchain interaction is consistent with our data. According to this approach, when the tethered chains are surrounded by a poor solvent, the chains will experience attractive tendencies, i.e., they will tend to become sticky. If the chains on adjacent particles interpenetrate on close approach, the attractive potential V_{steric} is given by eq 5, with the χ parameter exceeding $^1/_2$ (thus leading to a negative value for the potential). We can then differentiate eq 5 under the assumption that the octyl layer thickness L and segment volume fraction ϕ^{av} are effectively the same in all the liquids studied. The result can then be inserted into eq 8 to give the following correlation

$$G' \sim \left(\frac{1}{2} - \chi\right) \qquad (12)$$

This equation relates G' to the χ parameters for the octane−liquid pairs. Unfortunately, the χ parameter is not easily measured in such cases where the solvency is poor. We can however estimate its value using the solubility parameter approach. As given by eq 7, the χ parameter can be related to the solubility parameters of the surface chains (δ_s) and that of the medium (δ_m). To use this equation, we require values for the solubility parameters of the various media. These can be conveniently determined using a group contribution method as advanced by Hoy and van Krevelen.[33,34] We used this method to calculate δ values for the various liquids, and these are shown in Table 3 in units of $(MPa)^{1/2}$. We then used these values in eq 7 to obtain the χ parameter for each system (i.e., for *n*-octane in the corresponding liquid) and the resulting values of χ are provided in Table 4.

Note from Table 4 that in all cases the χ parameters exceed 0.5, thus pointing to the insolubility of the *n*-octyl chains in the polar liquids considered. This is encouraging and lends credibility to our approach. We then plot the gel moduli against $|(^1/_2 - \chi)|$ on a log−log plot as shown in Figure 14. We find that the data fall approximately on a straight line, thereby indicating a reasonably strong correlation between the two quantities. (The slope of the line is about 4/3, thereby indicating that the scaling relationship may not be exact.) More significantly, this approach is able to correctly capture all the trends observed in the rheological data, as can be ascertained from Table 4. Our analysis therefore suggests that the mixing interactions between surface chains are the most important in determining particle flocculation. As we have noted earlier, these interactions are attractive in our case because of the contact dissimilarity (i.e., difference in chemical nature) between the chain segments and the solvent medium. The implications of eq 12 are that if the mismatch between tethered chains and the medium is amplified (increase in χ), then the stickiness of the chains is correspondingly enhanced, leading to a denser network (higher gel modulus G'). Thus, if χ increases, so does the attractive interparticle potential, and hence so does G'.

In light of the above analysis, we can begin to comprehend the physical basis for the specific effects discussed in Figures 7−9, such as the effects of end-group and molecular weight. Since the *n*-octyl chains are nonpolar molecules, their miscibility in the liquid phase (i.e., χ) will be controlled by the polarity of the liquid molecules. In the case of polyether liquids, the −OH end-groups contribute significantly to the polarity of the molecules and dictate the extent of hydrogen bonding in the liquid phase. End-capping the PEG with methyl ($-CH_3$) groups reduces the polarity of the chain, and leads to a lower

Table 4. Experimental and Theoretical Parameters for R805 Silica Gels

system, R805 silica (*n*-octyl surface) dispersed in:	elastic modulus for 10% R805 gel G' at 1 rad/s (Pa)	effective Hamaker constant $A_{eff} = (\sqrt{A_m} - \sqrt{A_s})^2$ ($\times 10^{-21}$ J)	χ parameter for *n*-octane in liquid	$\lvert 1/2 - \chi \rvert$	effective solubility parameter term $\delta_{eff} = (\delta_s - \delta_m)^2$ (MPa)
EG3	22 000	1.35	10.11	9.61	149.6
PEG (300)	14 515	1.61	5.63	5.13	81.0
PEG-m (350)	6 344	1.29	3.21	2.71	43.8
PPG (425)	2 575	1.03	2.44	1.94	32.2
PEG-dm (250)	2 174	0.84	1.66	1.16	20.3
PPG (1000)	892	1.07	1.57	1.07	18.8
PPG (3000)	19[a]	1.08	1.25	0.75	13.9

[a] This data point is not included in Figures 13 and 14 because the system is not a true gel (see Figure 9 and corresponding text).

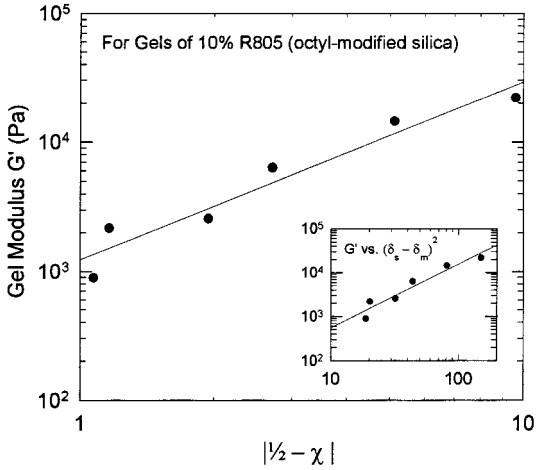

Figure 14. Test of the predicted scaling relationship between gel modulus (G') and the term involving the χ parameter. The data corresponds to the elastic modulus at 1 rad/s for gels of 10% R805 fumed silica in various liquids, extracted from Figures 7−9. The line drawn through the data has a slope of 4/3. The inset shows an equivalent scaling relationship between gel modulus and a term involving the mismatch in solubility parameter between the surface groups (δ_s) and bulk medium (δ_m).

solubility parameter (Table 3). Likewise, as the molecular weight of the polyether is increased, the influence of the −OH end-groups is decreased, and as a result, the solubility parameter decreases with molecular weight (Table 3). In each case, a lower δ value means a lower value of the χ parameter for the octane-liquid system (for example, end-capping reduces χ from 5.63 to 1.66 as seen from Table 4). The reduced χ implies an improved miscibility of octyl chains, and consequently a lower tendency to adhere to one another—and thereby a lower gel modulus.

In the above correlation, the dominant contribution arises from the solubility parameter mismatch. This can be seen clearly by rewriting eq 12 for the case where $\chi \gg 1/2$, and then incorporating eq 7 into the correlation, to yield:

$$G' \sim (\delta_s - \delta_m)^2 \tag{13}$$

In our case, χ does not strictly satisfy the above criterion over the range of liquids considered; nevertheless, a plot of eq 13 scales equally well as that due to eq 12 with regard to the quality of the regression fits (see inset of Figure 14). Values of the function $(\delta_s - \delta_m)^2$ are provided in Table 4. The above equation is quite useful from a practical standpoint. One can conceive of using this equation as an *a priori* test for gelation of particles bearing tethered chains. Qualitatively, eq 13 bears a distinct resemblance to eq 11, in that gelation is shown to arise due to the mismatch between tethered chains and continuous medium. The success of solubility parameters over Hamaker constants in quantifying this mismatch represents the significant finding from our study.[50]

To rationalize why the steric approach works while the vdW approach does not, let us examine the assumptions inherent in our analysis. Note that in evaluating the vdW potential V_{vdW} using the Vold model we treated the surface layer as a homogeneous shell of pure *n*-octane—i.e., we assumed the volume fraction ϕ^{av} of *n*-octyl segments in the surface layer to be equal to 1. As a result, the vdW potential function is confined to distances $d > 2L$ (V_{vdW} diverges at $d = 2L$), thereby suggesting that the layers can at best undergo surface adhesion. It is however more likely that the surface layer will be an inhomogeneous mixture of chains and solvent.[17,24,32] Even the presence of a few solvent molecules (or segments) within the bounds of the layer would affect the layer composition and would reduce the volume fraction ϕ^{av} of octyl segments in the layer to a value lower than 1. In fact, we might expect that the number of solvent molecules present within the layer (i.e., adjacent to the surface) would itself vary with solvent nature. Thus, solvent is expected to be increasingly included within the layer as we progress from highly polar (e.g., EG3) to less polar (e.g., PPG (3000)) media. In turn, the value of A_s for the surface layer has to account for the presence of solvent molecules within the layer in each case. This explains why the vdW approach cannot capture the trends in our data.

In contrast, the steric interactions become operational only when the particles are brought to a distance closer than $2L$, whereupon the surface chains are allowed to interpenetrate or overlap. Thus, the steric approach is a much more realistic representation of the interparticle interactions, and accurately captures the physics of the problem at close distances. At longer distances, the vdW interactions between the core particles may become important; however, these interactions are negligible in our systems (Figure 12). Within the interpenetration regime ($d < 2L$), it is not possible to apply the Hamaker theory for vdW forces, since it is a continuum theory which breaks down at the atomic level. In other words, in this regime, it is not possible to decouple V_{vdW} and V_{steric}.[51]

Support for the steric model can also be found from the studies of de Kruif, Russel, and co-workers on Stober silica particles bearing terminally attached stearyl (C_{18}) chains.[18−20] These particles form nonflocculated dispersions in alkanes (e.g., *n*-dodecane) at high temperatures but flocculate into gels on cooling. Gelation in these systems has been attributed to the same mechanism

(50) It is often suggested that χ scales with A_{eff}. The scaling between χ and A_{eff} only works for nonpolar systems where dispersive interactions dominate. In our systems, where the liquids are highly polar and capable of H-bonding, χ does not scale with A_{eff}.

(51) Fleer, G. J.; Cohen Stuart, M. A.; Scheutjens, J. M. H. M.; Cosgrove, T.; Vincent, B. *Polymers at interfaces*; Chapman & Hall: London, 1993.

invoked here—i.e., the overlap of chain segments on adjacent particles under conditions where the surrounding liquid is a poor solvent for the chains. In these studies, the solvent quality was varied by altering the *temperature*, whereas in our case, we have varied the *type of solvent*. The foregoing mechanism has been termed the sticky chains model by de Kruif,[19] and the particles are referred to as adhesive hard spheres.

Possible modifications to our analysis are now considered. In differentiating the steric potential (eq 7), we assumed that the segment volume fraction ϕ^{av} and layer thickness L are constants independent of the solvent nature. These assumptions may be invalid, especially for the case of thick polymeric layers. For example, the ϕ^{av} parameter may undergo significant changes as we progress from poor solvents to relatively better solvents, as has been observed experimentally through small angle neutron scattering (SANS).[46] Scope for refinement also exists with regard to the model we have used for relating G' to the pair potential. To predict G' quantitatively, and as a function of particle concentration, we need to account for the geometric details of the particles—in our case, the fractal nature of the fumed silica aggregates.

We finally consider our data on the R974 fumed silica which has both polar and nonpolar components on its surface: viz. the di-methyl groups (nonpolar) and the residual silanols (polar). Because of the complex surface chemistry, it is only possible to treat this silica in a qualitative fashion. The key to understanding the R974 silica is to note that it can exhibit either polar or nonpolar character, depending on the extent of mismatch between particle surface and liquid. The nonpolar methyl groups would tend to cluster together in highly polar media. On the other hand, the polar silanols (Si−OH) would tend to associate (possibly by a combination of H-bonding and dispersive interactions) in nonpolar media. Either of these processes could lead to flocculation and eventually to gel formation at high silica concentrations.

Our data indicates that the R974 silica is able to form gels in PEG, does not flocculate at all in PPG or in PEG-m, and flocculates weakly in PEG-dm (Figures 10 and 11). In the highly polar PEG, the nonpolar character of the R974 silica is evidenced. The PEG-m and PPG, however, are not polar enough to manifest the nonpolar nature of the R974 surface. At the same time, the −OH end-groups on these liquid molecules provide adequate polar character to suppress the attractive tendencies of the surface silanols on R974. In PEG-dm, both the −OHs are replaced, thereby reducing the liquid polarity and inducing some flocculation through the surface silanols. We can therefore consider the R974 silica to evince a split personality! In some instances, it shows polar (hydrophilic) character, while in others its hydrophobic tendencies dominate. Thus, the behavior of the R974 silica is considerably more complicated than that demonstrated by the R805 silica.

D. Conclusions

In this study we investigated a range of hydrophobic fumed silicas derived by attaching nonpolar *n*-alkyl chains to the silica surface. Silicas with long (C_8 or higher) tethered chains at high surface coverage were found to readily form gels in polar organic media. These gels were studied using dynamic rheology, with the objective of elucidating the colloidal interactions responsible for gel formation. We examined two possibilities for the controlling colloidal forces between the particles: (a) van der Waals interactions; and (b) chain stickiness caused by contact dissimilarity with solvent.

Based on our data, we believe there is compelling evidence for the latter possibility, implying that the flocculation process corresponds to a reverse of steric stabilization. The stickiness of surface chains is driven by their poor solvency in the continuous medium, and as the solvency deteriorates, the stickiness is enhanced, leading to a higher gel modulus. Accordingly, the gel modulus $G' \sim (\delta_s - \delta_m)^2$ i.e., it scales with a term involving the mismatch in solubility parameters between chain moieties and the solvent medium. This correlation between macroscopic properties to microstructure to colloidal interactions provides us with a rational basis for control of fumed silica microstructures in a given liquid.

Acknowledgment. We would like to thank Prof. Peter Kilpatrick, Department of Chemical Engineering, NCSU, for his helpful comments and criticisms on this work. This project was supported by the Department of Energy, Office of Basic Energy Sciences (BES) and, the Office of Transportation Technologies (OTT) through Lawrence Berkeley National Laboratories.

LA9815953